



OPEN

Enhancing procedural decision making with cone beam CT in renal artery embolization

Sung-Joon Park^{1,5}, Youngjong Cho^{2,5}, Hyoung Nam Lee³✉, Sangjoon Lee⁴, Hwan Hoon Chung¹ & Chan Ho Park³

Cone-beam computed tomography (CBCT) has proven to be a safe and effective adjunctive imaging tool for interventional radiology. Nevertheless, limited studies have examined the application of CBCT in renal artery embolization (RAE). The objective of this study is to evaluate the role of CBCT in intra-procedural decision-making for RAE. This multicenter retrospective study included 40 consecutive patients (age: 55.9 ± 16.5 years; male, 55%) who underwent CBCT during RAE from January 2019 to January 2023. The additional information provided by CBCT was classified into Category 1 (no additional information), Category 2 (more information without changing the treatment plan), and Category 3 (valuable information that led to a change in the treatment plan). CBCT did not add unique information for four patients (10%) classified as Category 1. CBCT clarified ambiguous angiographic findings and confirmed the existing treatment plan for 19 patients (47.5%) graded as Category 2; complex vascular anatomy was explained ($n = 13$), and a correlation between vascular territory and target lesion was established ($n = 6$). CBCT offered valuable information that was not visible on digital subtraction angiography and changed the treatment plan for 17 patients categorized as Category 3; a mismatch between the vascular territory and the target lesion led to the identification of alternative ($n = 3$) and additional feeders ($n = 8$); and the extent of embolization was reduced by using automatic feeder detection software ($n = 6$). CBCT is an efficient tool that aids in the decision-making process during the embolization procedure by providing supplementary imaging information. This additional information enables the confident identification of target vessels, facilitates superselective embolization, prevents non-target embolization, and helps locate missing feeders.

Renal artery embolization (RAE) is a minimally invasive therapeutic option used to treat a variety of renal disorders¹. It offers the advantage of protecting nephrons and having fewer serious complications than open surgeries. RAE is well-established as a first-line therapy for treating angiomyolipoma (AML)²⁻⁴. Adjunctive embolization and transarterial nephrectomy are increasingly utilized for patients requiring surgical nephrectomy^{5,6}. RAE controls acute renal hemorrhage due to spontaneous rupture, renal tumor, trauma, and iatrogenic injury^{7,8}. Endovascular treatment also plays an essential role in managing renal artery aneurysms and renal arteriovenous malformations (AVMs)^{9,10}.

Over the years, cone-beam computed tomography (CBCT) has proven to be a safe and effective adjunctive imaging tool for interventional radiology procedures such as trans-arterial chemoembolization (TACE), bronchial artery embolization and adrenal vein sampling¹¹⁻¹⁴. Nevertheless, limited studies have examined the application of CBCT in RAE. Previous research focused on the efficacy of CBCT in identifying feeders during tumor embolization¹⁵. However, it is important to note that CBCT has the potential to guide procedures in various situations beyond detecting tumor feeders.

Therefore, the purpose of this study was to evaluate the role of CBCT in making intra-procedural decisions for RAE performed for various conditions.

¹Department of Radiology, Korea University College of Medicine, Korea University Ansan Hospital, Ansan, Republic of Korea. ²Department of Radiology, University of Ulsan College of Medicine, Gangneung Asan Hospital, Gangneung, Republic of Korea. ³Department of Radiology, Soonchunhyang University College of Medicine, Cheonan Hospital, Cheonan, Republic of Korea. ⁴Vascular Center, The Eutteum Orthopedic Surgery Hospital, Paju, Republic of Korea. ⁵These authors contributed equally: Sung-Joon Park and Youngjong Cho. ✉email: radiology2010.hnl@gmail.com

Materials and methods

The Institutional Review Boards of all collaborating institutions approved this retrospective study and waived written informed consent for the use of clinical and imaging data. Written informed permission for interventional procedures was obtained from all patients. All methods were performed in accordance with the relevant guidelines and regulations.

Patients

The databases of three hospitals were queried from January 2019 to January 2023, and 40 consecutive patients (age: 55.9 ± 16.5 years; male, 55%) who underwent CBCT during RAE were identified. Table 1 summarizes the baseline characteristics of the study population. Indications for RAE were as follows: (1) control of acute renal hemorrhage ($n = 23$), (2) management of renal tumors ($n = 15$), and (3) embolization of renal artery aneurysm and AVM ($n = 2$). In all patients, contrast-enhanced abdomen or kidney CT was performed before the procedure. The decision to conduct endovascular therapy was determined through a multidisciplinary collaboration among a nephrologist, a urologist, and an interventional radiologist.

Angiography and embolization procedure

Computed tomography images were carefully reviewed before the procedure to identify the underlying etiology, evaluate the vascular anatomy, and predict the extent of parenchyma at risk. Patients underwent transcatheter angiography and embolization in an interventional procedure room equipped with one of the following commercially available angiography machines: AlluraClarity, AlluraXper (Philips Medical Systems), and Artis Q (Siemens Medical Systems). All the interventional procedures were performed in an inpatient setting by one of four board-certified interventional radiologists (S.P., Y.C., H.L. and H.C.). Each patient's vital signs were monitored throughout the procedure.

After local anesthesia with 2% lidocaine hydrochloride, transfemoral access was obtained under ultrasound guidance with a vascular sheath. A 5-Fr angled-tip angiographic catheter was employed during main renal angiographies. The contrast agent applied was Visipaque (iodixanol, 320 mg/mL, GE Healthcare). Based on the location of the target lesion, branching arteries were selectively catheterized using a coaxial 2.0–3.0-Fr microcatheter. Angiographies of extrarenal systemic arteries were also performed when necessary. Selective embolization was then attempted in all culprit arteries to avoid inadvertent embolization. The choice of embolic agent was entrusted to the attending physician's discretion.

Cone-beam computed tomography

The attending physician opted to perform CBCT before embolization for the following reasons: (1) a culprit artery or tumor feeder was not clearly delineated on digital subtraction angiography (DSA) ($n = 23$), (2) a target pathology was not opacified or partially opacified ($n = 14$), and (3) angiographic staining was ambiguous or uncertain ($n = 3$). CBCT was performed at the renal artery and/or extrarenal systemic artery. A microcatheter was utilized for selective CBCT when needed. A total of 5–30 mL of 50% diluted contrast medium was injected automatically at a rate of 0.5–3 mL/s according to the vessel diameter with a 4–6 s imaging delay. CBCT images were obtained during a breath-hold, with 5–6 s acquisition time covering a 200–240 rotation.

Acquired images were automatically transferred to one of the following 3-dimensional workstations: Interventional Workspot (Philips Medical Systems) and Leonardo Syngo X (Siemens Medical Systems). The embolization planning was supported by one of the following automated feeder detection (AFD) software: EmboGuide (Philips Medical Systems) and Syngo Embolization Guidance (Siemens Medical Systems). The results of the AFD software were then manually adjusted to add or delete vessels as needed.

Characteristic	Value
Age (years)	55.9 \pm 16.5
Male	22 (55%)
Right kidney	18 (45%)
Etiology	
Iatrogenic injury	14 (35%)
Angiomyolipoma	13 (32.5%)
Traumatic injury	8 (20%)
Renal cell carcinoma	2 (5%)
True aneurysm	1 (2.5%)
Arteriovenous malformation	1 (2.5%)
Spontaneous rupture	1 (2.5%)

Table 1. Baseline characteristics of the study population ($n = 40$). Continuous variables are presented as mean \pm standard deviation. Categorical variables are presented in absolute and relative frequencies (percentage).

Data analysis

The interventional radiologist who performed the procedure documented the DSA and CBCT findings, along with any changes to the treatment plan, in a procedure report. Each patient's imaging files, along with the corresponding procedure report, were retrospectively reviewed in chronological order of their acquisition by three other interventional radiologists who did not participate in the original procedure. Based on the additional information provided by CBCT, the reviewers assigned each case to one of three categories: Category 1 = CBCT provided no additional information; Category 2 = CBCT provided more information without changing the treatment plan; Category 3 = CBCT provided valuable information that led to a change in the treatment plan. The criteria for each category are summarized in Table 2. Any differences of opinion were resolved by mutual review and consensus.

Anatomical variations of the renal artery were categorized into three types, including early branching (the first renal branch arises within 1.5 cm of the renal artery ostium), accessory artery (enters the kidney from the hilum along with the main renal artery), and aberrant artery (enter the kidney directly from the capsule outside the hilum)^{16,17}. The embolization level was categorized as a main renal, divisional, segmental, interlobar, capsular, or extrarenal artery. The embolization extent was graded according to the embolized vascular territory: grade 1 = less than one segment; grade 2 = less than two segments; grade 3 = less than three segments; and grade 4 = less than four segments¹⁸.

The clinical and laboratory data, including age, gender, etiology, and serum creatinine concentrations, were collected from the patient's electronic medical records. According to the guidelines of the Kidney Disease Improving Global Outcomes, post-procedural acute kidney injury (AKI) was defined as an escalation in serum creatinine concentration of ≥ 0.3 mg/dL (26.5 μ mol/L) or a $\geq 50\%$ increase within 48 h^{18,19}. The remaining procedural complications were classified as either major or minor according to the guidelines of the Society of Interventional Radiology²⁰.

Results

The details of 40 procedures are summarized in Table 3. The target lesion was located in the left kidney in 22 patients and the right kidney in 18 patients. Each renal angiogram illustrated normal anatomy in 34 patients, accessory arteries in three patients (Fig. 1), early branching in two patients, and an aberrant artery in one patient. A single CBCT scan was performed for 35 patients, whereas two CBCT scans were performed for five patients. A total of 45 CBCT scans were performed with the catheter tip placed in the main ($n = 38$), divisional ($n = 1$), segmental ($n = 3$), and extra-renal arteries ($n = 3$). The extra-renal arteries included the right inferior phrenic and adrenal arteries, which supplied the tumor, as well as the left adrenal artery, which was involved in an iatrogenic vascular injury. CBCT was performed in two patients without enhancement to verify lipiodol uptake after the procedure; however, these data were not incorporated into the imaging analysis.

The embolized arteries were segmental ($n = 17$), interlobar ($n = 23$), capsular ($n = 3$), and extra-renal arteries ($n = 3$). The embolic materials included coil ($n = 24$), N-butyl cyanoacrylate (NBCA) with iodized oil ($n = 10$), ethanol with iodized oil ($n = 7$), polyvinyl alcohol ($n = 4$), microsphere ($n = 3$), and Gelfoam ($n = 3$). The extent of embolization was grade 1 in 29 patients (72.5%), grade 2 in six patients (15%), grade 3 in four patients (10%), and grade 4 in one patient (2.5%). Two patients experienced post-procedural AKI with embolization extents graded as 3 and 4, respectively. Serum creatinine concentrations returned to baseline within two days after the procedure. There were no other major or minor procedural complications.

CBCT did not add unique information for four patients (10%) graded as Category 1. CBCT clarified inconclusive angiographic findings and confirmed the existing treatment plan for 19 patients (47.5%) classified as Category 2. In 13 patients, CBCT helped explain the complex vascular anatomy caused by vascular overlap and arteriovenous fistulas (Fig. 2). A correlation between vascular territory and the target lesion was established in six patients in whom the target lesion was not apparent on DSA (Fig. 3). CBCT offered valuable information that was not visible on DSA and changed the treatment plan for 17 patients (42.5%) noted as Category 3. A mismatch between the vascular territory and the target lesion led to the identification of alternative ($n = 3$) and additional (including extra-renal) feeders ($n = 8$). The extent of embolization was reduced in six patients by using AFD software.

Category 1	CBCT provided no additional information
Added no unique information beyond the DSA findings	
Category 2	CBCT provided more information without changing the treatment plan
Clarified questionable findings observed on DSA	
Established a correlation between vascular territory and the target lesion	
Category 3	CBCT provided valuable information that led to a change in the treatment plan
Led to the embolization of additional renal or extra-renal arteries	
Led to the catheterization of alternative renal arteries after normal tissue staining	
Led to the reduction of embolization extent using AFD software	

Table 2. Interpretive categories and criteria for CBCT for renal artery embolization. CBCT, cone-beam computed tomography; DSA, digital subtraction angiography; AFD, automated feeder detection.

Characteristic	Value
Number of CBCT scans	
1 scan	35 (87.5%)
2 scans	5 (12.5%)
Level of CBCT angiography	
Main artery	38 (95%)
Divisional artery	1 (2.5%)
Segmental artery	3 (7.5%)
Extra-renal artery	3 (7.5%)
Level of embolization	
Segmental artery	17 (42.5%)
Interlobar artery	23 (57.5%)
Capsular artery	3 (7.5%)
Extra-renal artery	3 (7.5%)
Embolic material	
Coil	24 (60%)
NBCA with iodized oil	10 (25%)
Ethanol with iodized oil	7 (17.5%)
Polyvinyl alcohol	4 (10%)
Microsphere	3 (7.5%)
Gelfoam	3 (7.5%)
Multiple agents	10 (25%)
Extent of embolization	
Grade 1	29 (72.5%)
Grade 2	6 (15%)
Grade 3	4 (10%)
Grade 4	1 (2.5%)

Table 3. Summary of procedural details ($n=40$). CBCT, cone-beam computed tomography; NBCA, *N*-butyl cyanoacrylate.

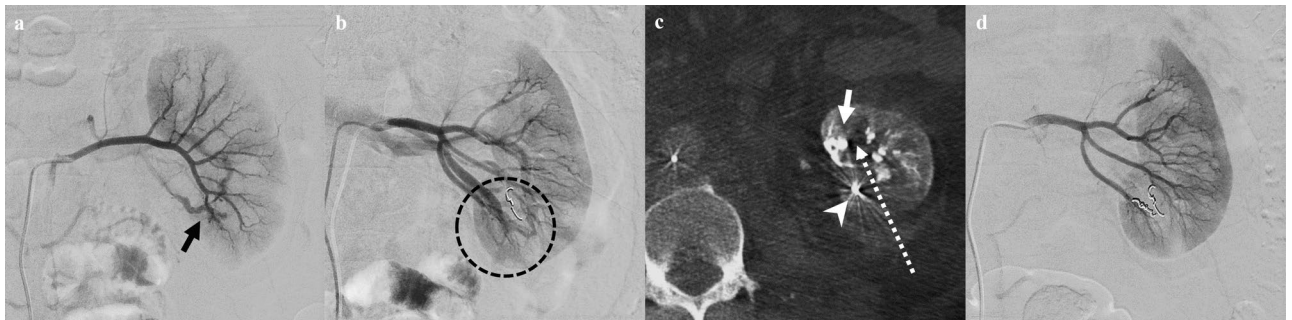


Figure 1. A 45-year-old male patient with hematuria following percutaneous renal biopsy. (a) Angiography of the left renal artery reveals rapid venous filling contrast medium, which suggests an arteriovenous fistula (arrow) at the lower pole. Coil embolization was performed. (b) Angiography of the accessory renal artery demonstrates rapid filling of the renal venous system, suggesting another arteriovenous fistula (circle). (c) Cone-beam CT confirms an arteriovenous fistula (arrow), indicating another injury from the biopsy needle. A coil is also noted from a previous embolization (arrowhead). The dashed arrow indicates the approximate direction of the biopsy needle. (d) Post-embolization angiography displays no evidence of remnant arteriovenous fistula.

Discussion

The DSA technique facilitates optimal visualization of the vascular structure, which is crucial for evaluating target lesions and guiding the endovascular guidewire and catheter. However, interpreting DSA can be challenging due to various factors, such as overlapping structures and insufficient tumor vascularity. As a result, obtaining a comprehensive view of the blood vessels may require repeat angiographies at different projections. Kothary et al.²¹ demonstrated that CBCT could replace multiple angiographic runs during TACE, resulting in a negligible increase in the total dose-area product while reducing the use of contrast media. This multicenter retrospective study involved 40 consecutive patients who underwent CBCT-guided RAE. Among them, CBCT helped

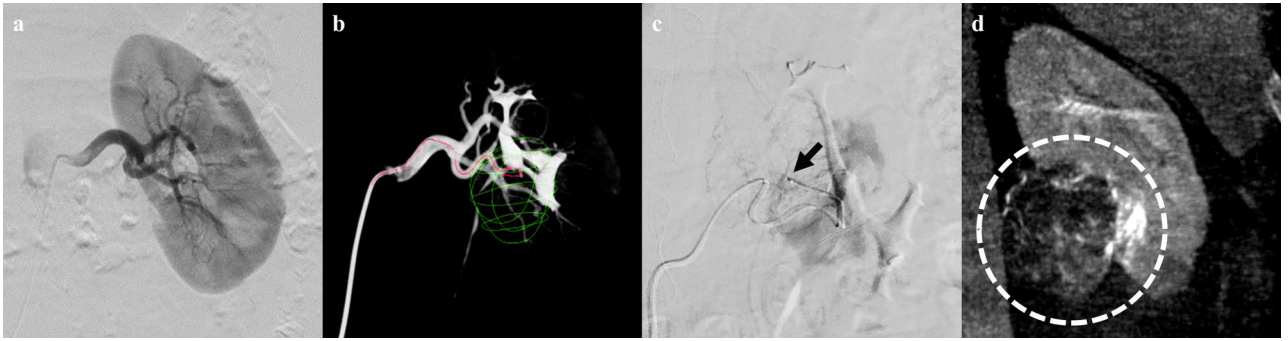


Figure 2. A 56-year-old male patient with an incidentally discovered renal angiomyolipoma. (a) Angiography of the left renal artery reveals no apparent tumor staining, and no tumor feeder can be identified. (b) Automated feeder detection software identifies the vessel pathway (red line) leading to the tumor (green lines). (c) Spot image exhibits the successful positioning of the microcatheter tip (arrow) at the feeding artery during embolization, which was performed using a mixture of absolute ethanol and iodized oil. (d) CBCT immediately after embolization demonstrates iodized oil accumulation in the tumor (circle).

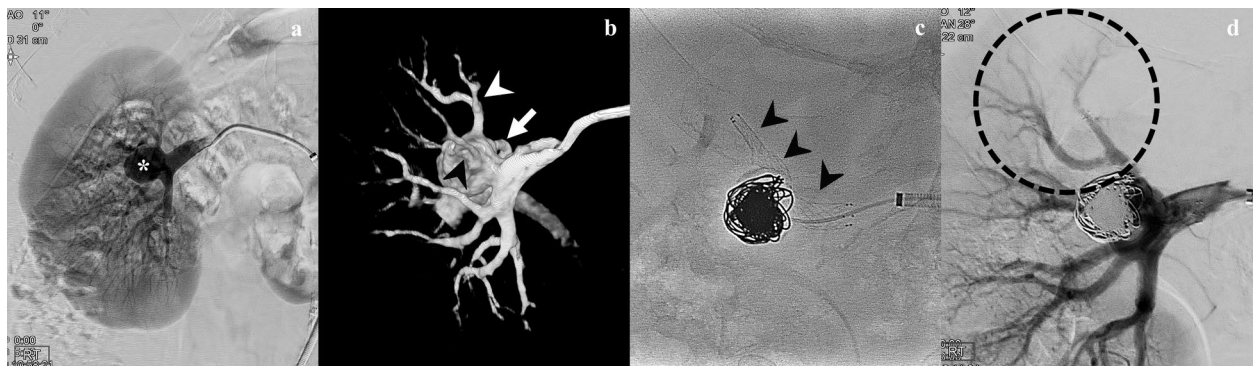


Figure 3. A 61-year-old male patient who underwent stent-assisted coil embolization for renal artery aneurysm. (a) Angiography of the right renal artery reveals a wide-necked hilar renal artery aneurysm (asterisk). The aneurysm and the renal arterial branches overlap, making it difficult to differentiate one from the other. (b) The volume-rendered image demonstrates that the aneurysm involves apical (white arrowhead), superior anterior (black arrowhead), and posterior (white arrow) segmental branches. (c) Spot image displays the insertion of a bare metal stent (black arrows) during coil embolization to prevent ischemia of the apical and posterior segments. (d) Post-embolization angiography indicates good exclusion of the aneurysm while preserving the flow of the parent branch (circle).

clarify inconclusive angiographic findings and confirmed the existing treatment plan in 19 patients (47.5%). Furthermore, CBCT provided valuable information that was not detected by DSA, leading to a modification of the treatment plan in 17 patients (42.5%).

Utilization of CBCT for evaluation of the renal artery had several advantages over the assessment of the hepatic artery or other visceral arteries. According to the previous study employing CBCT during TACE, the image quality of the left lateral segment was poorer than that of the other segments due to cardiac motion²². Moreover, the quality of CBCT images varies significantly depending on the patient's respiratory coordination. CBCT renal arteriography is less susceptible to motion artifacts because the kidney is a retroperitoneal organ near the axial skeleton. As a second point, the kidney is a small enough organ to be included in the field of view (FOV) of CBCT. As a result, CBCT can provide anatomical information about the entire kidney with a single acquisition. Conversely, the previous study stated that CBCT could encompass the entire liver within the FOV in only 29% of cases^{11,22}.

There has been extensive research on using CBCT to guide transcatheter treatments for hepatic malignancies^{23,24}. In this study, CBCT was also beneficial for detecting tumor feeders and providing therapeutic guidance during RAE. The hallmark imaging features of hepatocellular carcinoma are arterial phase hyperenhancement and portal/delayed washout. On the other hand, AML consists of blood vessels, smooth muscle, and fat in varying proportions, resulting in various imaging features and enhancement patterns^{25–27}. Hypervascular tumors display apparent staining on DSA, but there are also tumors with poor vascularity that are difficult to identify. In this context, the role of CBCT in establishing a correlation between vascular area and target lesion is helpful in practical terms. Furthermore, AFD software was beneficial for identifying fine feeders, enabling superselective embolization of the segmental or interlobar branches.

In this study, acute renal hemorrhage caused by iatrogenic or traumatic injury was the most common etiology. RAE is an effective method for the control of bleeding, irrespective of the cause. Despite its advantages, ischemic renal parenchymal injury is a major concern after RAE. Embolization may cause renal ischemia or infarction in a large portion of the kidney, depending on the location of the vascular injury. The risk of post-procedural AKI was found to be significantly lower in patients with less than one segment of ischemic injury¹⁸. Our experience suggests that AFD software was also noteworthy in pinpointing the fine branch responsible for the hemorrhage, leading to a reduction in embolization extent than relying on DSA alone.

Based on the characteristics of the target lesion, various embolic agents can be used for RAE. In this study, the hemostatic procedure was performed using coil and NBCA as the main embolic agents, and ethanol was frequently used to embolize AML. Compared to other embolic agents, ethanol has several attractive properties for use in the management of AML^{2,4}. This liquid embolic agent penetrates the capillary bed level and induces protein denaturation, resulting in permanent tumor damage. Alternatively, non-target embolization can cause severe damage to normal tissue and should be avoided. As a result, despite its many advantages, ethanol is not commonly used as a primary embolic agent. In our experience, CBCT on vessels where ethanol embolization is planned greatly enhanced operator confidence by accurately evaluating the vascular territory²⁸.

The presence of extrarenal feeding vessels is not uncommon, especially if the diameter and volume of the AML are large²⁹. AMLs can be supplied by extrarenal branches from the renal artery (e.g., the renal capsular artery and the inferior adrenal artery) or the aortic arch (e.g., the middle adrenal artery, the lumbar artery, the intercostal artery, and the inferior mesenteric artery)³⁰. In patients with renal injury, concomitant injuries of the extrarenal vessel have been described not only after trauma but also after iatrogenic injury^{31,32}. Incomplete embolization of extrarenal culprit arteries can lead to tumor regrowth or rebleeding. Although CT and DSA imaging help recognize extrarenal vessels, determining their presence is sometimes difficult. CBCT can assist in confirming and guiding the procedure to avoid suboptimal embolization.

Previous studies have described a variety of endovascular techniques for managing renal aneurysms and AVMs^{23–25}. The choice of treatment strategy depends on the location, angiographic type, and architecture of the target lesion⁹. In this study, CBCT was instrumental in determining the optimal technique and selecting a suitable interventional device. For instance, CBCT confirmed the exact location of aneurysmal neck and branches arising from the parent vessel in a patient with a wide-necked renal artery aneurysm³³. By placing the bare metal stent in the optimal location, coil migration could be successfully prevented. For renal AVMs, CBCT guided the superselection of multiple feeding arteries with AFD software, and it was possible to place the microcatheter as close to the nidus as possible³⁴.

This study has several limitations that should be noted. First, there may have been potential selection bias. The decision to perform CBCT was at the discretion of the attending physician. Second, the retrospective review of medical records prevented a detailed evaluation of records such as radiation exposures and contrast medium requirement data. Third, the computed tomography protocols, including slice thickness, tube current, and enhancement phase, were not standardized due to the multicenter study design. Fourth, the study population was small.

In conclusion, CBCT is an efficient tool that aids in the decision-making process during the embolization procedure by providing supplementary imaging information. This additional information enables the confident identification of target vessels, facilitates superselective embolization, prevents non-target embolization, and helps locate missing feeders.

Data availability

The data that support the findings of this study are available from the corresponding author, upon reasonable request.

Received: 7 June 2024; Accepted: 5 August 2024

Published online: 06 August 2024

References

- Muller, A. & Rouvière, O. Renal artery embolization—indications, technical approaches and outcomes. *Nat. Rev. Nephrol.* **11**, 288–301 (2015).
- Lee, S. *et al.* Radiologic and clinical results of transarterial ethanol embolization for renal angiomyolipoma. *Eur. Radiol.* **31**, 6568–6577 (2021).
- Hocquet, A. *et al.* Long-term results of preventive embolization of renal angiomyolipomas: Evaluation of predictive factors of volume decrease. *Eur. Radiol.* **24**, 1785 (2014).
- Lee, W. *et al.* Renal angiomyolipoma: Embolotherapy with a mixture of alcohol and iodized oil. *J. Vasc. Interv. Radiol. JVIR* **9**, 255–261 (1998).
- Schwartz, M. J., Smith, E. B., Trost, D. W. & Vaughan, E. D. Renal artery embolization: Clinical indications and experience from over 100 cases. *BJU Int.* **99**, 881–886 (2007).
- Choe, J. *et al.* Safety and efficacy of transarterial nephrectomy as an alternative to surgical nephrectomy. *Korean J. Radiol.* **15**, 472–480 (2014).
- Mohsen, T., El-Assmy, A. & El-Diasty, T. Long-term functional and morphological effects of transcatheter arterial embolization of traumatic renal vascular injury. *BJU Int.* **101**, 473–477 (2008).
- Wang, H. L., Xu, C. Y., Wang, H. H. & Xu, W. Emergency transcatheter arterial embolization for acute renal hemorrhage. *Med. Baltim.* **94**, e1667 (2015).
- Hwang, J. H. *et al.* Embolization of congenital renal arteriovenous malformations using ethanol and coil depending on angiographic types. *J. Vasc. Interv. Radiol. JVIR* **28**, 64–70 (2017).
- Ma, T. *et al.* Mid-term results of coil embolization alone and stent-assisted coil embolization for renal artery aneurysms. *Ann. Vasc. Surg.* **73**, 296–302 (2021).
- Kim, H.-C. Role of C-arm cone-beam CT in chemoembolization for hepatocellular carcinoma. *Korean J. Radiol.* **16**, 114–124 (2015).

12. Cho, Y., Lee, S. & Park, S.-J. Effectiveness of intraprocedural dual-phase cone-beam computed tomography in detecting hepatocellular carcinoma and improving treatment outcomes following conventional transarterial chemoembolization. *PLoS One* **16**, e0245911 (2021).
13. Liu, M. Y. *et al.* Utility of cone-beam CT for bronchial artery embolization and chemoembolization: A single-institution retrospective case series. *Cardiovasc. Intervent. Radiol.* **45**, 834–840 (2022).
14. Meyrignac, O. *et al.* Impact of cone beam—CT on adrenal vein sampling in primary aldosteronism. *Eur. J. Radiol.* **124**, 108792 (2020).
15. Kim, M. S. *et al.* Performance of cone-beam computed tomography (CBCT) renal arteriography for renal tumor embolization. *Eur. J. Radiol.* **157**, 110598 (2022).
16. Leckie, A. *et al.* The renal vasculature: What the radiologist needs to know. *Radiogr. Rev. Publ. Radiol. Soc. N. Am. Inc.* **42**, 80 (2022).
17. Kumar, S., Neyaz, Z. & Gupta, A. The utility of 64 channel multidetector CT angiography for evaluating the renal vascular anatomy and possible variations: A pictorial essay. *Korean J. Radiol.* **11**, 346–354 (2010).
18. Lee, H. N. *et al.* Impact of superselective renal artery embolization on renal function and blood pressure. *J. Belg. Soc. Radiol.* **104**, 59 (2020).
19. Levin, A. *et al.* Kidney Disease: Improving Global Outcomes (KDIGO) CKD Work Group. KDIGO 2012 clinical practice guideline for the evaluation and management of chronic kidney disease. *Kidney Int. Suppl.* **3**, 1–150 (2013).
20. Khalilzadeh, O. *et al.* Proposal of a new adverse event classification by the society of interventional radiology standards of practice committee. *J. Vasc. Interv. Radiol. JVIR* **28**, 1432–1437.e3 (2017).
21. Kothary, N. *et al.* Imaging guidance with C-arm CT: Prospective evaluation of its impact on patient radiation exposure during transhepatic arterial chemoembolization. *J. Vasc. Interv. Radiol. JVIR* **22**, 1535–1543 (2011).
22. Lee, I. J. *et al.* Cone-beam CT hepatic arteriography in chemoembolization for hepatocellular carcinoma: Angiographic image quality and its determining factors. *J. Vasc. Interv. Radiol. JVIR* **25**, 1369–1379 (2014).
23. Kim, H.-C. *et al.* Transcatheter arterial chemoembolization for hepatocellular carcinoma: Prospective assessment of the right inferior phrenic artery with C-arm CT. *J. Vasc. Interv. Radiol. JVIR* **20**, 888–895 (2009).
24. Kim, H.-C. *et al.* Intercostal artery supplying hepatocellular carcinoma: Demonstration of a tumor feeder by C-arm CT and multidetector row CT. *Cardiovasc. Intervent. Radiol.* **34**, 87–91 (2011).
25. Jinzaki, M. *et al.* Renal angiomyolipoma: A radiological classification and update on recent developments in diagnosis and management. *Abdom. Imaging* **39**, 588–604 (2014).
26. Park, B. K. Renal angiomyolipoma: Radiologic classification and imaging features according to the amount of fat. *AJR Am. J. Roentgenol.* **209**, 826–835 (2017).
27. Song, S., Park, B. K. & Park, J. J. New radiologic classification of renal angiomyolipomas. *Eur. J. Radiol.* **85**, 1835–1842 (2016).
28. Durack, J. C. *et al.* Assessment of automated cone-beam CT vessel identification software during transarterial hepatic embolization: Radiation dose, contrast medium volume, processing time, and operator perspectives compared to digital subtraction angiography. *Clin. Radiol.* **73**(1057), e1-1057.e6 (2018).
29. Zhang, X. *et al.* Can we predict the existence of extrarenal feeders to renal angiomyolipomas? *Eur. Radiol.* **29**, 2499–2506 (2019).
30. Jung, Y., Choi, M. J., Kim, B. M., Kim, Y. M. & Seo, Y. Transarterial embolization for sporadic renal angiomyolipoma: Patient selection and technical considerations for optimal therapeutic outcomes. *J. Korean Soc. Radiol.* **83**, 559–581 (2022).
31. Fuchigami, J. *et al.* Development of ileocolic artery pseudoaneurysm after renal biopsy. *Radiol. Case Rep.* **17**, 4413–4416 (2022).
32. Ngho, C. L. Y., Wee, B. B. K. & Wong, W. K. Lumbar artery bleed as a complication of percutaneous renal biopsy and a proposed workflow for massive bleeding. *Case Rep. Nephrol. Dial.* **8**, 268–276 (2018).
33. Das, J. P. *et al.* Balloon-assisted coil embolization (BACE) of a wide-necked renal artery aneurysm using the intracranial sceptor C compliant occlusion balloon catheter. *CVIR Endovasc.* **1**, 12 (2018).
34. Lee, S. Y. *et al.* Efficacy and safety of transvenous embolization of type II renal arteriovenous malformations with coils. *J. Vasc. Interv. Radiol. JVIR* **30**, 807–812 (2019).

Author contributions

All authors conceptualized the study. S.P., Y.C., and H.L. developed the methodology. Formal analysis and investigation were conducted by S.P., Y.C., and H.L. The original draft was prepared by S.P. and Y.C. All authors reviewed and edited the manuscript. H.L. supervised the study.

Funding

This work was supported by the Soonchunhyang University Research Fund. This research did not receive any specific grant from funding agencies in the public, commercial, or not-for-profit sectors.

Competing interests

The authors declare no competing interests.

Additional information

Correspondence and requests for materials should be addressed to H.L.

Reprints and permissions information is available at www.nature.com/reprints.

Publisher's note Springer Nature remains neutral with regard to jurisdictional claims in published maps and institutional affiliations.

Open Access This article is licensed under a Creative Commons Attribution-NonCommercial-NoDerivatives 4.0 International License, which permits any non-commercial use, sharing, distribution and reproduction in any medium or format, as long as you give appropriate credit to the original author(s) and the source, provide a link to the Creative Commons licence, and indicate if you modified the licensed material. You do not have permission under this licence to share adapted material derived from this article or parts of it. The images or other third party material in this article are included in the article's Creative Commons licence, unless indicated otherwise in a credit line to the material. If material is not included in the article's Creative Commons licence and your intended use is not permitted by statutory regulation or exceeds the permitted use, you will need to obtain permission directly from the copyright holder. To view a copy of this licence, visit <http://creativecommons.org/licenses/by-nc-nd/4.0/>.

© The Author(s) 2024